DEVELOPMENT AND CHARACTERIZATION OF ELECTROSPUN SILK FIBROIN SCAFFOLDS REINFORCED WITH GOLD NANOPARTICLES

[1]Y. MONTOYA, [2]A. GARCÍA-GARCÍA, [3]J. BUSTAMANTE

[1,3] Grupo de Dinámica Cardiovascular, Línea Ingeniería de Tejidos y Protésica Cardiovascular, Universidad Pontificia Bolivariana, Medellín, Colombia
[3]Comité de Trabajo de Bioingeniería Cardiovascular, Sociedad Colombiana de Cardiología y Cirugía Cardiovascular, Bogotá, Colombia.
[2]Centro de InvestigaciónenMaterialesAvanzados, S.C. (CIMAV), Subsede Monterrey, Av. Alianza Norte 202, Parque PIIT, Apodaca, Nuevo León CP 66628, Mexico
E-mail: yuliet.montoya@upb.edu.co

Abstract - Developments in the field of nanotechnology have made it possible to harness the physical and chemical properties of nanomaterials; in this regard, some nanoparticles are being targeted for applications in the diagnosis and treatment of various pathologies. In this field, various biomaterials of natural or synthetic origin developed currently can incorporate biologically active components to define complex and dynamic interactions that promote and regulate the events occurring in a cellular microenvironment. This research focused on the development of a polymeric scaffold reinforced with gold nanoparticles to determine its morphological, physical, chemical, and electrical properties. The results showed three-dimensional fibrillar structures with fiber diameters ranging from 74 to 98 nm, which were reinforced with gold nanoparticles with a tendency toward sphericity and diameters between 11 and 14 nm. In addition, the presence of functional groups such as CO, CH, amide A, I, II, and III was determined, demonstrating the interaction between silk fibroin, the synthetic polymer, and gold nanoparticles, obtained from biosynthesis with silk fibroin. Furthermore, scaffolds functionalized with gold nanoparticles show increased electrical conductivity due to a smaller filament diameter that increases the contact surface and causes electrons to move more quickly. Due to their functional characteristics, these nanostructured scaffolds could be candidates for use in generating bioelectrical connection bridges in the field of biomedical engineering.

Keywords - Bioactive Scaffold, Gold Nanoparticles, Silk Fibroin, Synthetic Polymer

I. INTRODUCCIÓN

Among the manufacturing processes of nanoparticles, there is the synthesis by chemical reduction of ionic salts with or without the presence of stabilizing agents, where the reducing agent through the donation of electrons favors the reduction of ions, in this case of $Au^{3+}$and $Ag^{+}$to $Au^{0}$and Ag^{0}oxidation states, as a result of the capture of the donated electrons and their subsequent reduction.[1].

Most synthesis methods through chemical reduction make use of highly reactive reducing agents such as sodium borohydride($NaHB_4$) [2], hydrazine (N_2H_4) [3] (CH_2O) [4],where the presence of chemical traces in the final compound converts them into toxic by-products, making them unsuitable for biomedical applications[5]. Therefore, the use of environmentally and biologically biocompatible reducing agents is becoming a new alternative. These include proteins and peptides, which, in addition to promoting the formation of nanostructures based on the presence of one or more specific amino acids, in most cases confer colloidal stability and greater biocompatibility to the material. Among these is silk fibroin, a protein extracted from silk fibers, derived from silkworms such as Bombyx mori[6].

The recent integration of nanotechnology in the field of medicine has allowed the use of the physicochemical properties inherent to different materials at the nanometric scale, in order to propose new therapeutic methodologies, such as controlled drug release[7], cell therapy techniques [8], tissue repair[9]and microbial control[10], focused on improving the quality of life of the population.

n the search for a biomaterial with a biocompatible response, some natural biopolymers have been studied, among which is silk fibroin (SF). This protein can be obtained from sericultural fibrous waste, which is mainly constituted by SF. This is a structural protein that has been shown to be biocompatible and of controllable biodegradability, which exhibits mechanical properties superior to those of other natural biopolymers such as collagen, which is why SF is considered a material of interest to use in the field of cardiovascular tissue engineering [11][12]. In addition to the above, the versatility of fibroin to be processed in aqueous and organic systems is added, as well as the ease with which it can be chemically modified, which has made it an applicable material in the biomedical and pharmaceutical industries [13][14].

The use of nanostructured materials for biomedical engineering applications is a topic that is just

beginning to be seen as alternative therapeutic methods. Therefore, itisnecessarytodevelop new processesthatallowtheproductionofnanostructureswith lowcytotoxicity, withcontrolledsize and shape, highpurity and in environmentallyfriendlyconditions[16]. To mitigate this behavior, the use of functionalization processes is required, generally with elements of natural origin, giving rise to biocomposite materials, as is the case of the use of polymers as a support matrix for nanoparticles for the possible treatment of wounds[17]r as an antibacterial agent [18].

In this context, this research was oriented towards the development and physical, chemical, and electrical characterization of an electrospun bioactive scaffold composed of silk fibroin, extracted from Colombian sericultural waste, and reinforced with gold nanoparticles, obtained by green synthesis, for applications such as nanostructured materials with a high degree of biocompatibility.

II. DETAILS EXPERMIENTAL

2.1 Extractionofsilkfibroin

Silk fibroin was obtained using silk waste purchased from the Cauca Sericulture Development Corporation (CORSEDA). To obtain silk fibroin, the sample was degummed by immersion in an aqueousNa_2CO_3 solution with continuous stirring. The sample was then dissolved in a 9.3 M LiBr aqueous solution with constant stirring. The solution was dialyzed until stable conductivity was achieved, and then centrifuged. Finally, the silk fibroin concentration was determined.

2.2 Synthesisofgoldnanoparticles

Silk fibroin was used at0.5 % v/v, and chloroauric acid $HAuCl_4$ a 2.5 mM with pH adjustment to 10 with 0.1 N sodium hydroxide. The solution was incubated with 60 W LED light, at a temperature between32 - 34° C.

2.3 Electrospinning of gold nanoparticle-reinforced membranes

SFw was used atSF_w at 4.8 % v/v y óxido de polietileno (PEO) de 4 % m/v and gold nanoparticles (AuNPs-SF) at 100% v/v. A polymer blend was carried out at a volumetric ratio of 50/25/25 (PEO/SF/AuNPs-SF). The solution was electrospun in a rotational collector at 250 rpm at a voltage of 15 kV, at a distance of20 cm,and a flow rate 0.7 mL/h. The scaffolds were treated with 90% v/v and washed for 24 h with distilled water at 37ºC to remove the PEO.

2.4 Scanning and field-scanning transmission electron microscopy

The morphological characteristics and size of the gold nanoparticles were analyzed using a FEI Nova NanoSEM 200 field emission scanning electron microscope in STEM mode at 15 kV. In addition, the fiber size of the scaffolds was determined using a Nova NanoSEM 200 field emission scanning electron microscope and a JEOL JSM-6490LV scanning electron microscope operated at 15 kV.

2.5 Ultraviolet-visible spectrometry

To determine the formation of gold nanoparticles and their incorporation into the scaffolds, an Agilent UV-Vis-NIR Cary 5000 spectrophotometer was used, in a wavelength range between 1100 – 200 nm.

2.6 Fourier transforminfraredspectroscopy

Regarding the changes in the functional groups present in the membrane, a Nicolet iS50 spectrometer with an attenuated total reflectance module was used at a resolution of 4 cm^{-1} and 32 scans. The infrared spectra obtained were used to determine the percentage of secondary structures present in the amide I of the membranes.

2.7 Electrochemicalimpedancespectroscopy

The electrospun membranes were evaluated using electrochemical impedance spectroscopy to determine their electroconductive properties. Para losregistros se empleó un potenciostatoIviumn IviumCompactStatpotentiostat was used for recording sweeping frequencies ranging from 0 Hz a 500 kHz with 10 points per decade and 160 mV de amplitud del potencial AC. potential amplitude. The resistivity and conductivity of the material were determined using equations 1 and 2

$$\rho = R\frac{S}{l} \quad \text{(Eq. 1)} \qquad \sigma = \frac{1}{\rho} \quad \text{(Eq. 2)}$$

Whereρis the electrical resistivity, Ris the electrical resistance, Sis the cross section of the scaffold with and without nanoparticles, lis the length, andσis the electrical conductivity.

2.8 Kelvin Probe Force Microscopy (KPFM)

To determine the topography and potential differential of the surface of the electrospun membrane with nanoparticles, an Asylum Research brand atomic force microscope and a silicon tip withTi/Ir (5/20) coating with a radius 28 ± 10 nm, model ASYELEC-01.

III. RESULTS AND DISCUSSION

3.1 Morphological analysis of nanoparticle-reinforced electrospun scaffolds

Fig. 1a shows the absorption spectrum corresponding to the surface plasmon resonance (SPR), where the resonance generated by the increase in the movement of free electrons in the conduction band of the surface of the nanoparticles, allowed to show the spectral band located at a wavelength between 522 – 528 nm, which is related to characteristic resonances for gold nanoparticles.[19].

Table 1.Particle size, polydispersity index, and electrokinetic potential of gold and silver nanoparticles, of gold nanoparticles using SF as a reducing agent.

Samplet ype	SPR (nm)	Particlesize(nm)	PDI	Zeta Potential(mV)
AuNPs-SF	525 ±2	11.5±2.5	0.04 8	- 40.2±1.5

In Fig. 2b, the micrograph of the gold nanoparticles synthesized with SF (AuNPs-SF) at 0.5 % v/v is shown, where an average particle diameter of 11.5 ± 2.5 was found, denoting a higher population density of nanoparticles and a polydispersity index (PDI) close to zero, which indicates that the gold nanoparticles have uniform and monodisperse sizes (Table 1).Regarding the colloidal stability provided by silk fibroin to gold nanoparticles, it was found that nanostructures with pH values greater than the isoelectric point of SF (Ip 4.58 – 5.00), exhibit colloidal stability, due to the charge repulsion presented by the completely deprotonated acid groups and the beginning of the deprotonation of the amino groups betweenpI – pKa[20].

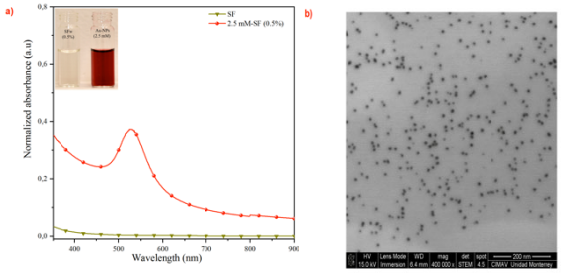

Fig. 1. Gold nanoparticles using silk fibroin as a reducing and stabilizing agent. a) UV-visible spectrum and b) STEM micrograph. Scale: 200 nm.

The electrospinning and post-treatment process resulted in an electrospun membrane with continuous fibers and nanometer-scale filament diameters (78 ± 24 nm). STEM micrographs allowed the identification of the AuNPs-SF without agglomerations in the fibrillar structure of the scaffold.(Fig. 2b).

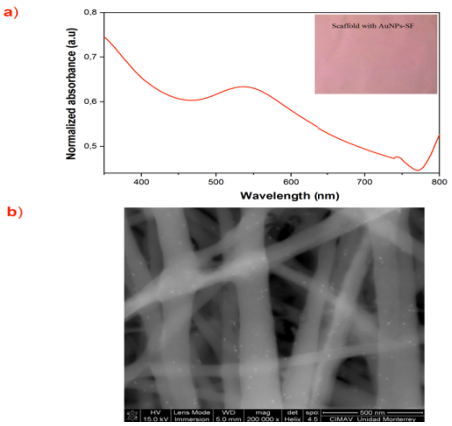

Fig. 2. Electrospun scaffold reinforced with AuNPS-SF. Where a) UV-visible spectrum and b) SEM micrograph. Scale 500 nm.

The electrospun membranes functionalized with AuNPs-SF showed absorption spectra corresponding to the surface plasmon resonance for the gold ion. Furthermore, the color of the membranes turned pink for those electrospun with AuNPs-SFw (Fig. 2a).

3.2 FTIR

The FTIR spectra in Fig. 3 show the conformational chemical changes of the functional groups of the AuNPs-SF electrospun membranes after post-treatment with 90 % MeOH.In the spectra, the presence of absorption bands at wavelengths of 3286 cm^{-1}, 1638 cm^{-1}, 1528 cm^{-1} and 1241 cm^{-1}, was observed, characteristic peaks of amide A (N-H stretching), amide I(C=O stretching), amide II (N–H bending and C–N stretching) and amide III (C–C, C–N stretching and C–H bending), related to the contribution of SF[21]. On the other hand, in the scaffolds treated with MeOH a reduction in the absorption bands was evident at2880 cm^{-1} (aliphatic stretchingC-H), 1001 cm^{-1} (stretchingC-O), 957 cm^{-1} (C-H out of plane) and840 cm^{-1} (C-H out of plane), which correspond to the synthetic sacrificial polymer (PEO).

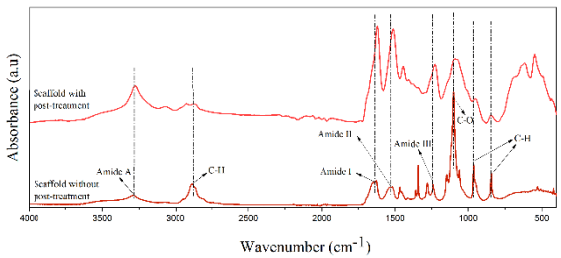

Fig. 3FTIR spectra of AuNPs-SF reinforced scaffolds without and with90 % v/v methanol post-treatment.

3.3 Electrical analysis of the AuNPs-SF reinforced scaffold

From equations 1 and 2, the electrical behavior of the electrospun membranes functionalized with AuNPs-SF was determined. In Fig. 4a, it is evident that the

electrospun scaffolds without AuNPs presented a resistivity of8,993 Ω*cm, while the fibrillar structures reinforced with the nanostructures exhibited resistivity values of5650 Ω*cm. This indicates that the resistivity of the material decreases when containing in its structure a network of fibers with gold nanoparticles, which favors a greater alignment of the fibers and a uniform distribution of[22].

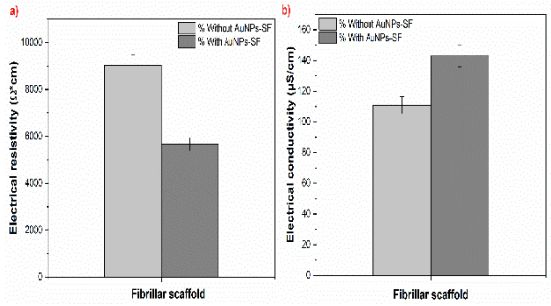

Fig. 4.Electrical behavior of electrospun SF membranes reinforced with gold nanoparticles. Where a) electrical resistivity and b) electrical conductivity. SF membranes without nanoparticles were used as controls.

On the other hand, Fig. 4b shows the electrical conductivity of the scaffolds without and with nanoparticles with values of111 µS/cm and 142 µS/cm, respectivamente. respectively. The conductivity is given by the capacity of the material to conduct an electric current through it, when analyzing the results obtained from the membranes reinforced with nanoparticles, it is indicated that by incorporating metals such as gold in the atomic and molecular structure of the electrospun membranes, an increase in conductivity is observed, behavior that could be due to a high number of electrons with weak interactions, which facilitates their movement in the structure of the electrospun scaffolds[23]. Furthermore, a smaller filament diameter causes an increase in electrical conductivity, since the contact surface area increases and the electrons can move more easily[24].

3.4 KPFM Analysis

Fig. 5a shows the topography of the scaffold without post-treatment, where homogeneous fibers and the presence of defects can be observed, likewise, the contact potential differential is shown with values between 0.10 V and 0.25 V. After the treatment process, the scaffold reinforced with gold nanoparticles, it was found that a fibrillar morphology is preserved with apparently smaller and more homogeneous diameters, and when comparing the height of the topography with the untreated scaffold, it was observed that it decreased from 2.94 µm to 1 µm. This decrease is due to the extraction of PEO from the electrospun membrane, which was present in 50 % of the final structure of the scaffold(Fig. 5b).

On the other hand, the surface potential differential of the MeOH-treated membrane went from presenting a positive to a negative potential with values between- 0.237 V and - 0.554 V; the change in the difference in surface potential could be directly correlated with the change in the chemistry of the electrospun membrane surface, which when treated with MeOH exposes negatively charged amino acids such as aspartic and glutamic acid on the surface[25].

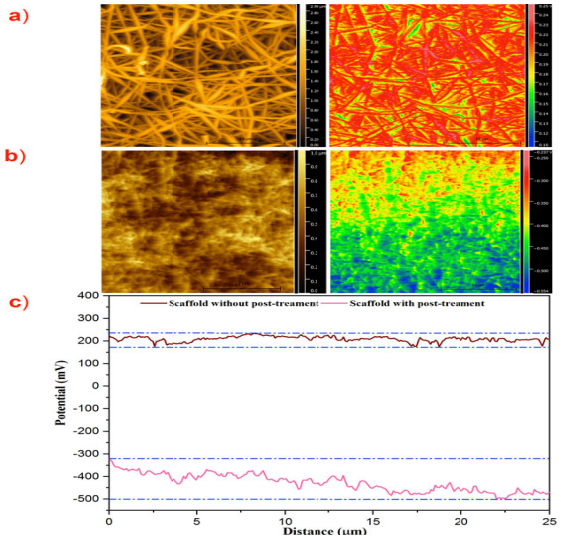

Fig. 5.AFM and KPFM of a membrane without MeOH treatment, where a) topography and surface potential. Membrane with MeOH treatment, where b) topography and surface potential, and c) surface potential profiles of the membranes without and with nanoparticles and without and with MeOH treatment.

Fig. 5c shows the behavior of the electrical potential (mV) versus the position (mV) of the scaffold reinforced with AuNPs with and without treatment. In the upper part of the graph, the variation of the surface potential can be observed with minimum valuesof 0.18 V and with a maximum peak at 0.22 V or the untreated membrane and a difference between both of 61 mV. While, in the lower part is the variation of the surface potential of the treated membrane, which presents minimum values at - 0.66 V and maximum at- 0.52 V,and a difference between both of- 0.13 V. Based on the results, it is inferred that these signals are modified due to electrostatic interactions at an atomic scale and short-range forces possibly caused by the generation of charged ionic species, which could conduct an electrical stimulus as a result of the change in the polarity of the scaffold[26].

IV. CONCLUSIONS

The use of silk fibroin in aqueous solution at low concentrations allowed the production of electrospun scaffolds using polyethylene oxide and gold nanoparticles as a support material and modifier of the apparent viscosity and conductivity values of the solutions.

Gold nanoparticle-reinforced scaffolds were obtained with a continuous fibrillar morphology, uniform fiber

diameters, and absence of structural defects. These scaffolds behave as dielectric components when not reinforced with nanoparticles, but when gold nanostructures are incorporated, they become charge carriers, facilitating the conduction of electrical stimuli.

Finally, the topographic and surface potential results obtained by KPFM indicate that the interweaving of fibers in post-treated gold nanoparticle scaffolds present a beneficial topographic signal for tissue engineering, as they can serve as a conductive biomimetic tool.

ACKNOWLEDGMENTS

To the Ministry of Science, Technology and Innovation-Minciencias and the Sistema General de Regalías – SGR for the grant number BPIN2020000100190 for supported this research and the Center for Research in Advanced Materials (CIMAV).

REFERENCES

[1] B. Bhattarai, Y. Zaker, and T. P. Bigioni, “Green synthesis of gold and silver nanoparticles: Challenges and opportunities,” Current Opinion in Green and Sustainable Chemistry, vol. 12, pp. 91–100, 2018, doi: 10.1016/j.cogsc.2018.06.007.

[2] S. Wojtysiak and A. Kudelski, “Influence of oxygen on the process of formation of silver nanoparticles during citrate/borohydride synthesis of silver sols,” Colloids and Surfaces A: Physicochemical and Engineering Aspects, vol. 410, pp. 45–51, 2012, doi: 10.1016/j.colsurfa.2012.06.012.

[3] V. Dugandžić, I. J. Hidi, K. Weber, D. Cialla-May, and J. Popp, “In situ hydrazine reduced silver colloid synthesis – Enhancing SERS reproducibility,” Analytica Chimica Acta, vol. 946, pp. 73–79, 2016, doi: 10.1016/j.aca.2016.10.018.

[4] N. Wang, Y. Liu, Y. Li, Q. Liu, and M. Xie, “Fluorescent and colorimetric sensor for Cu 2+ ion based on formaldehyde modified hyperbranched polyethylenimine capped gold nanoparticles,” Sensors and Actuators, B: Chemical, vol. 255, pp. 78–86, 2018, doi: 10.1016/j.snb.2017.08.035.

[5] H. Duan, D. Wang, and Y. Li, “Green chemistry for nanoparticle synthesis,” Chemical Society Reviews, vol. 44, no. 16, pp. 5778–5792, 2015, doi: 10.1039/c4cs00363b.

[6] E. Afjeh-Dana et al., “Gold nanorods reinforced silk fibroin nanocomposite for peripheral nerve tissue engineering applications,” International Journal of Biological Macromolecules, vol. 129, pp. 1034–1039, 2019, doi: 10.1016/j.ijbiomac.2019.02.050.

[7] Y. K. Kurokawa and S. C. George, “Tissue engineering the cardiac microenvironment: Multicellular microphysiological systems for drug screening,” Advanced Drug Delivery Reviews, vol. 96, pp. 225–233, 2016, doi: 10.1016/j.addr.2015.07.004.

[8] G. Bodelón, C. Costas, J. Pérez-Juste, I. Pastoriza-Santos, and L. M. Liz-Marzán, “Gold nanoparticles for regulation of cell function and behavior,” Nano Today, vol. 13, pp. 40–60, 2017, doi: 10.1016/j.nantod.2016.12.014.

[9] B. Subia, T. Dey, S. Sharma, and S. C. Kundu, “Target specific delivery of anticancer drug in silk fibroin based 3D distribution model of bone-breast cancer cells,” ACS Applied Materials and Interfaces, vol. 7, no. 4, pp. 2269–2279, 2015, doi: 10.1021/am506094c.

[10] H. Soliman, A. Elsayed, and A. Dyaa, “ Antimicrobial activity of silver nanoparticles biosynthesised by Rhodotorulasp . strain ATL72 ,” Egyptian Journal of Basic and Applied Sciences, vol. 5, no. 3, pp. 228–233, 2018, doi: 10.1016/j.ejbas.2018.05.005.

[11] H. Liu, X. Li, G. Zhou, H. Fan, and Y. Fan, “Electrospun sulfated silk fibroin nanofibrous scaffolds for vascular tissue engineering,” Biomaterials, vol. 32, no. 15, pp. 3784–3793, May 2011, doi: 10.1016/j.biomaterials.2011.02.002.

[12] H. Park et al., “Silk fibroin–polyurethane blends: Physical properties and effect of silk fibroin content on viscoelasticity, biocompatibility and myoblast differentiation,” Acta Biomaterialia, vol. 9, no. 11, pp. 8962–8971, Nov. 2013, doi: 10.1016/j.actbio.2013.07.013.

[13] P. Sensharma, G. Madhumathi, R. D. Jayant, and A. K. Jaiswal, “Biomaterials and cells for neural tissue engineering: Current choices.,” Materials science & engineering. C, Materials for biological applications, vol. 77, pp. 1302–1315, 2017, doi: 10.1016/j.msec.2017.03.264.

[14] R. You, Y. Xu, G. Liu, Y. Liu, X. Li, and M. Li, “Regulating the degradation rate of silk fibroin films through changing the genipin crosslinking degree,” Polymer Degradation and Stability, vol. 109, pp. 226–232, 2014, doi: 10.1016/j.polymdegradstab.2014.07.029.

[15] I. Khan, K. Saeed, and I. Khan, “Nanoparticles: Properties, applications and toxicities,” Arabian Journal of Chemistry, 2017, doi: 10.1016/j.arabjc.2017.05.011.

[16] [16] J. Polte, “Fundamental growth principles of colloidal metal nanoparticles - a new perspective,” CrystEngComm, vol. 17, no. 36, pp. 6809–6830, 2015, doi: 10.1039/c5ce01014d.

[17] [17] M. G. Mehrabani, R. Karimian, B. Mehramouz, M. Rahimi, and H. S. Kafil, “Preparation of biocompatible and biodegradable silk fibroin/chitin/silver nanoparticles 3D scaffolds as a bandage for antimicrobial wound dressing,” International Journal of Biological Macromolecules, vol. 114, pp. 961–971, 2018, doi: 10.1016/J.IJBIOMAC.2018.03.128.

[18] C. S. Shivananda, B. L. Rao, A. Pasha, and Y. Sangappa, “Synthesis of Silver Nanoparticles Using Bombyxmori Silk Fibroin and Their Antibacterial Activity,” IOP Conference Series: Materials Science and Engineering, vol. 149, no. 1, 2016, doi: 10.1088/1757-899X/149/1/012175.

[19] Q. Shou, C. Guo, L. Yang, L. Jia, C. Liu, and H. Liu, “Effect of pH on the single-step synthesis of gold nanoparticles using PEO–PPO–PEO triblock copolymers in aqueous media,” Journal of Colloid and Interface Science, vol. 363, no. 2, pp. 481–489, Nov. 2011, doi: 10.1016/j.jcis.2011.07.021.

[20] W. S. Denham and W. Brash, “47—THE ISOELECTRIC POINT OF SILK-FIBROIN,” Journal of the Textile Institute Transactions, vol. 18, no. 10,

pp. T520–T525, Jan. 1927, doi: 10.1080/19447022708661437.

[21] B. N. Singh, N. N. Panda, and K. Pramanik, "A novel electrospinning approach to fabricate high strength aqueous silk fibroin nanofibers," International Journal of Biological Macromolecules, vol. 87, pp. 201–207, Jun. 2016, doi: 10.1016/j.ijbiomac.2016.01.120.

[22] S. Jin, J. Yu, Y. Zheng, W.-Y. Wang, B. Xin, and C.-W. Kan, "Preparation and Characterization of Electrospun PAN/PSA Carbonized Nanofibers: Experiment and Simulation Study," Nanomaterials, vol. 8, no. 10, p. 821, Oct. 2018, doi: 10.3390/nano8100821.

[23] D. Chen, Y.-E. Miao, and T. Liu, "Electrically Conductive Polyaniline/Polyimide Nanofiber Membranes Prepared via a Combination of Electrospinning and Subsequent In situ Polymerization Growth," ACS Applied Materials & Interfaces, vol. 5, no. 4, pp. 1206–1212, Feb. 2013, doi: 10.1021/am303292y.

[24] K. Dincer, "INVESTIGATION OF ELECTRICAL CONDUCTIVITY OF NANOFIBERS (PAN) CONTAINING NANOPARTICLES (GRAPHENE, COPPER, SILICA) PRODUCED BY ELECTROSPINNING METHOD," 2018.

[25] T. Busoloet al., "Surface potential tailoring of PMMA fibers by electrospinning for enhanced triboelectric performance," Nano Energy, vol. 57, pp. 500–506, Mar. 2019, doi: 10.1016/j.nanoen.2018.12.037.

[26] B. Tulachanet al., "Electricity from the Silk Cocoon Membrane," Scientific Reports, vol. 4, no. 1, p. 5434, May 2015, doi: 10.1038/srep05434.

★★★